Proc. Natl. Acad. Sci. USA
Vol. 89, pp. 1109–1112, February 1992
Biophysics

Direct measurement of brain glucose concentrations in humans by ^{13}C NMR spectroscopy

(glucose transport/blood–brain barrier/*in vivo* NMR/glucose metabolism)

ROLF GRUETTER*†, EDWARD J. NOVOTNY‡, SUSAN D. BOULWARE‡, DOUGLAS L. ROTHMAN§, GRAEME F. MASON*, GERALD I. SHULMAN§, ROBERT G. SHULMAN*, AND WILLIAM V. TAMBORLANE‡

Departments of *Molecular Biophysics and Biochemistry, ‡Pediatrics, and §Internal Medicine, Yale University School of Medicine, New Haven, CT 06510

Contributed by Robert G. Shulman, November 8, 1991

ABSTRACT **Glucose is the main fuel for energy metabolism in the normal human brain. It is generally assumed that glucose transport into the brain is not rate-limiting for metabolism. Since brain glucose concentrations cannot be determined directly by radiotracer techniques, we used ^{13}C NMR spectroscopy after infusing enriched D-[1-^{13}C]glucose to measure brain glucose concentrations at euglycemia and at hyperglycemia (range, 4.5–12.1 mM) in six healthy children (13–16 years old). Brain glucose concentrations averaged 1.0 ± 0.1 μmol/ml at euglycemia (4.7 ± 0.3 mM plasma) and 1.8–2.7 μmol/ml at hyperglycemia (7.3–12.1 mM plasma). Michaelis–Menten parameters of transport were calculated to be K_t = 6.2 ± 1.7 mM and T_{max} = 1.2 ± 0.1 μmol/g·min from the relationship between plasma and brain glucose concentrations. The brain glucose concentrations and transport constants are consistent with transport not being rate-limiting for resting brain metabolism at plasma levels >3 mM.**

Under normal conditions, brain cells rely almost entirely on the availability of D-glucose for generation of energy. The lack of significant carbohydrate stores in the brain requires that a steady glucose supply from the blood be maintained. However, D-glucose cannot diffuse freely across the blood–brain barrier but is transported by facilitated diffusion (1–4) mediated by specific transporter molecules (5–7). The importance of glucose transport to metabolism and brain function has spurred extensive research in animals (for reviews, see refs. 8 and 9), as well as in humans (10, 11). Although the rate of glucose transport is considered to be rapid enough to meet the cellular energy demand under basal conditions, it may become rate-limiting during hypoglycemia (11, 12). Alterations in brain glucose transport may also be involved in the central nervous system morbidity associated with diseases such as diabetes mellitus, seizures, or hypoxic–ischemic encephalopathy (13, 14).

Glucose transport into the brain can be evaluated by measuring brain glucose concentrations as a function of plasma levels (15, 16). Direct measurement of glucose concentration is possible in animal brain with rapid-freezing techniques (17, 18). However, these *in vitro* methods cannot be applied to humans, and direct quantitation of human brain glucose concentration has thus far not been achieved.

NMR spectroscopy has been shown to be a powerful noninvasive technique that can be used to determine the concentration of many metabolites in living tissue (19–23). Recent studies have shown that the α- and β-anomers of glucose can be measured in animal brain by ^{13}C NMR, when D-[1-^{13}C] glucose is infused (16, 24). We report here the quantitation of the glucose concentration in the human brain using localized ^{13}C NMR spectroscopy and the determination of the kinetic parameters of D-glucose transport from the relationship between brain and plasma glucose concentration.

METHODS

Six nonobese healthy children (13–16 years old) were studied after written informed consent was obtained from the subjects and their parents using forms and procedures approved by the Yale Human Investigations Committee. Sensory stimulation was minimized by having the subjects wear ear plugs and an eye mask.

Glucose levels and fractional enrichment (Fig. 1) were controlled by using the glucose insulin clamp technique (25, 26) as follows: The fractional enrichment of [1-^{13}C]glucose (percentage of total plasma glucose) was increased in the blood by infusing initially 15 g of 99% enriched D-[1-^{13}C]glucose in a 20% (wt/vol) solution into the left antecubital vein. After 10 min, the infusion was switched to a 50% enriched dextrose infusate in order to minimize variations in the fractional enrichment in blood during the study. Plasma glucose concentration was maintained at the hyperglycemic plateau by adjusting the infusion rate of glucose based on blood samples (25) obtained from the right arm every 5 min during the study and measured immediately in a Beckman glucose analyzer. The drop in plasma glucose was achieved by stopping the glucose infusion. A primed continuous insulin infusion (0.5 milliunits/kg·min; Humulin; Eli-Lilly, Indianapolis) was started during the hyperglycemia period in order to suppress endogenous hepatic production of unlabeled glucose. The 50% [1-^{13}C]glucose infusion was resumed in order to maintain steady levels at euglycemia (4.8 mM).

The fractional enrichment was measured in samples obtained every 10 min by gas chromatography/mass spectrometry of the pentaacetate derivatives of plasma glucose after deproteinization and deionization (26). Additional deproteinized samples obtained at specific time points were analyzed by ^1H NMR at 360 MHz in ^2H_2O to determine the degree of enrichment at the C1 position.

The subjects were supine in a 2.1-Tesla whole body magnet (ORS-Bruker, Billerica, MA) on a double surface coil consisting of a 7-cm-diameter ^{13}C coil and a concentric 14-cm ^1H coil. A vol of 144 ml (6 × 4 × 6 cm) was localized within the occipitoparietal region of the brain that excluded major blood vessels and the ventricles, based on inversion recovery ^1H magnetic resonance images obtained just before the start of the infusion [repetition time (TR) = 2500 ms; inversion time (TI) = 800 ms; echo time (TE) = 14 ms]. Spectrometer adjustments were performed during the initial increase in plasma glucose (Fig. 1). The rf power was adjusted on a 2-cm

The publication costs of this article were defrayed in part by page charge payment. This article must therefore be hereby marked "*advertisement*" in accordance with 18 U.S.C. §1734 solely to indicate this fact.

Abbreviation: NOE, nuclear Overhauser effect.

†To whom reprint requests should be addressed at: Department of Molecular Biophysics and Biochemistry, MRC 126, Yale University, 333 Cedar Street, P.O. Box 3333, New Haven, CT 06510.

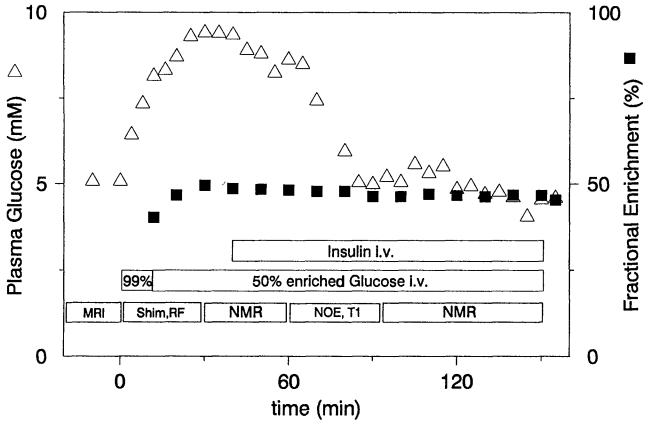

FIG. 1. Infusion protocol and time course of the concentration and ^{13}C fractional enrichment of glucose in plasma during a typical study. Horizontal bars indicate the protocol: The time of insulin infusion (top); variable-rate glucose infusion at different enrichment levels (middle); and times used for positioning (MRI; magnetic resonance image), spectrometer adjustments (Shim, RF), correction factors (NOE, T1), and the localized ^{13}C NMR measurements (NMR), which are shown in Fig. 2*B*. In this study, the SD during either NMR measurement was 0.5 mM for the average plasma glucose concentration and 0.3% at euglycemia and 0.6% at hyperglycemia for the fractional enrichment.

sphere at the coil center containing an aqueous solution of [^{13}C]formic acid. The power for the ^{13}C coil was adjusted to give a 150-μs 180° pulse. The ^{1}H decoupling power was set for a 900-μs 90° pulse by minimizing the ^{13}C NMR signal of the sphere with the sequence 90°(^{13}C) − $1/2J$ − θ(^{1}H) − acquire (^{13}C) (27). The 90° pulse duration used for decoupling was set to 1.2 ms. Adjusting rf power rather than pulse durations had the advantage that the flip angle distribution in space did not vary from study to study. Localized shimming of all first- and second-order shim coils was achieved with an automated sequence (28).

The localization was based on the image-selected *in vivo* spectroscopy (ISIS) technique (29), where 8-ms-long hyperbolic secant pulses were used for magnetization inversion (19) and a 5-ms adiabatic half passage sin/cos pulse with a numerically optimized modulation function was used for excitation. (For pulse simulations, see ref. 30.) To minimize the z magnetization and to ensure proper localization, the pulse used for excitation was applied again at the end of the acquisition (31). During the signal acquisition time of 102 ms, WALTZ-16 proton broadband decoupling (32) was used with a power of at most 13 W. The glucose signal intensity was increased with nuclear Overhauser effect (NOE) enhancement generated by 1 W of continuous wave irradiation at 4.9 ppm in the ^{1}H NMR spectrum during the recovery delay of 1.5 s. The maximum tissue rf power deposition was calculated to be below 2 W/kg when a magnetic vector potential model was used (33).

The spectra were zero-filled to 408 ms, multiplied with an exponential function corresponding to 5-Hz line broadening. Fourier transformed, and phase corrected, and the baseline was corrected between 85 and 105 ppm. Peak areas were determined by summation from 93.3 to 92.0 ppm (α-glucose at 92.76 ppm) and from 97.0 to 96.0 ppm (β-glucose at 96.6 ppm).

RESULTS

The appearance of [1-^{13}C]glucose in the head was monitored in unlocalized spectra at a 2-min time resolution, one of which is shown in Fig. 2*A* (bottom). Localized ^{13}C NMR measurements were acquired in 4-min blocks (TR = 1.7 s; 128 averages) and signals summed during 30 min of constant hyper- and euglycemia (Fig. 1) are shown in Fig. 2*B*. The linewidths were typically between 2 and 3 Hz when correcting for the 5-Hz exponential multiplication.

Brain D-[1-^{13}C]glucose concentrations were determined by comparing the integrals of the localized *in vivo* signals to those obtained under identical experimental conditions from a phantom solution containing 270 mM D-glucose (equivalent to 3 mM D-[1-^{13}C]glucose at natural abundance, 50 mM KCl, and 2 mM NaN_3). The measurements were corrected for the influence of coil loading (19) and the combined effect of NOE and T_1 relaxation on the signal strength. The effect of loading was measured by integrating the upfield peak of the formate doublet in separate fully relaxed spectra obtained from the small sphere placed at the coil center. These corrections were small (10–20%). The combined effect of NOE and T_1 was assessed in unlocalized spectra by determining the ratio of the glucose signals obtained with NOE generation by using the parameters of the localization experiment (TR = 1.7 s) to that of the signal obtained under fully relaxed conditions (TR

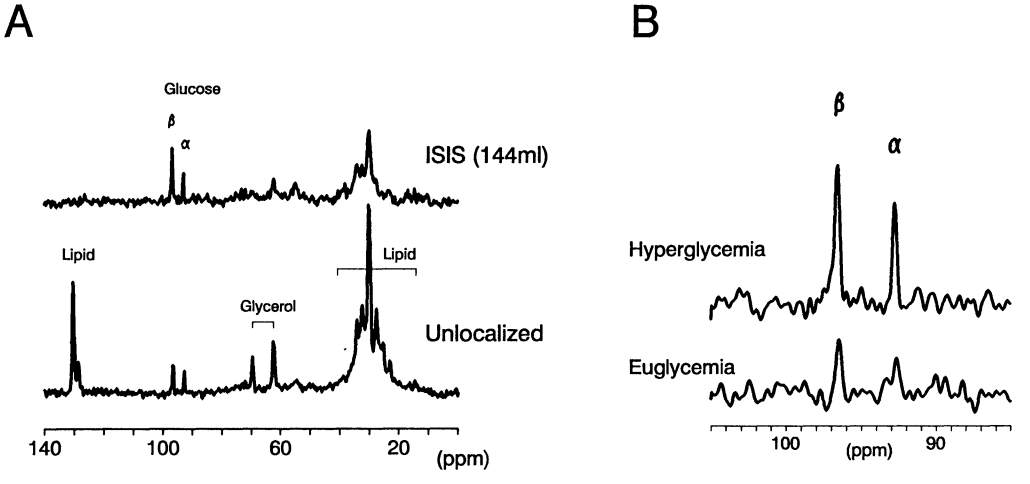

FIG. 2. Experimental spectra of D-[1-^{13}C]glucose in the human brain. (*A*) Lower trace, expansion from an unlocalized spectrum acquired in 2 min (TR = 1.7 s; 64 averages) showing, in addition to the peaks of α- and β-glucose, signals from lipid primarily in the scalp. The peaks on either side of the glucose resonances—i.e., the C2 peak of the glycerol backbone at 69.7 ppm and the fatty acyl peaks at 130 ppm, vanish upon localization as shown in the upper trace, indicating localization of the glucose signals within the brain. (*B*) Upper trace, localized spectrum acquired during hyperglycemia (30 min; 1024 averages) at 8.4 mM plasma concentration; lower trace (30 min, 1024 averages), collected during the euglycemia period (4.8 mM plasma) as indicated in Fig. 1. Both spectra are shown with the same vertical scale.

= 5.2 s) in the absence of NOE generation. To minimize transient effects during the fall of glucose *in vivo*, these measurements were interlaced by concurrent alternation of the recovery delay and NOE generation. To obtain the total intracerebral concentration, the resulting concentrations of [1-^{13}C]glucose in the brain were divided by the fractional enrichment of [1-^{13}C]glucose in plasma averaged during the time required for the localized NMR measurements. The resulting brain glucose concentrations are plotted in Fig. 3 versus the average plasma glucose concentration during the measurement period. The stability of plasma glucose was judged based on the standard deviation of plasma glucose during the localized NMR measurements. The deviations averaged at 0.3 mM with the extreme at 0.5 mM. The fractional enrichment variations were <0.035 during any 30 min of NMR measurements with an average of the 12 measurement periods at 0.48 ± 0.07 (mean ± SD).

The symmetric Michaelis–Menten model, which is described in the legend of Fig. 3, was used to calculate the kinetic parameters of glucose transport into the brain. This model has been validated in animals (7, 8, 34) and assumes (*i*) that the rate-limiting step for glucose entry into the brain is at the capillary endothelial cells comprising the blood–brain barrier, (*ii*) that intra- and extracellular brain glucose concentrations are the same, and (*iii*) that glucose transport across both sides of capillary endothelia exhibit the same Michaelis–Menten kinetics with maximum unidirectional transport rates of T_{max} and half-maximal transport rates at glucose concentrations of K_t.

Prior to the fit of the model (Eq. **1** in Fig. 3 legend), brain glucose concentrations (expressed in μmol per ml of brain vol) were divided by the aqueous fraction of brain space—i.e., 0.77 (34)—assuming a specific gravity of 1 g/ml for brain tissue. The standard Levenberg–Marquardt algorithm was used for nonlinear least-squares fitting of Eq. **1** to the experimental data in Fig. 3. Errors were determined by a Monte-Carlo simulation—i.e., by adding random gaussian noise to the best fit at the plasma levels measured (35). The rms amplitude of the simulated noise was set to the estimated rms error of the brain glucose measurements. T_{max} was

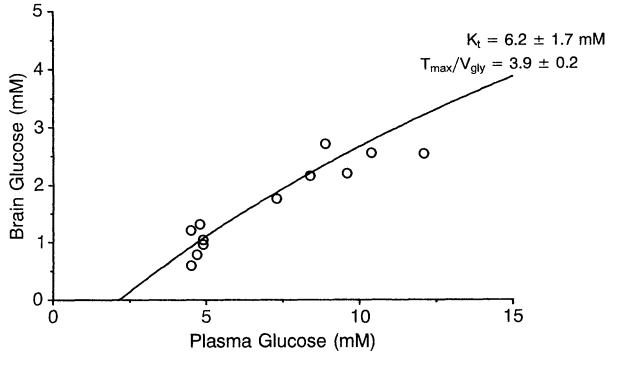

FIG. 3. Determination of the kinetic parameters from the brain glucose concentrations (μmol per ml of brain vol) measured at euglycemia and hyperglycemia in six normal individuals. The model requires that at steady state the rate of glucose influx across the blood–brain barrier, T_{in}, equals the sum of the rate of efflux, T_{out}, plus the rate of metabolism, V_{gly}. If T_{in} and T_{out} are assumed to have the same Michaelis–Menten kinetics (8, 15, 34), the steady-state relationship between brain and blood glucose concentrations is given by ($x = [\text{glucose}_{plasma}]/K_t$; $v = T_{max}/V_{gly}$)

$$[\text{glucose}_{brain}] = K_t \times \{[x(v - 1) - 1]/(x + 1 + v)\}. \quad [1]$$

This equation was fitted to the data points (solid line) as in previous studies (15, 16) of animals in order to calculate the apparent Michaelis–Menten constant of transport, K_t, as well as the ratio T_{max}/V_{gly} of the apparent maximal glucose transport rate, T_{max}, to the glucose consumption rate V_{gly}.

calculated from the ratio T_{max}/V_{gly}, assuming the steady-state glycolytic rate V_{gly} to be a constant value of 0.3 μmol/g·min, based on observations that arteriovenous glucose differences do not depend on the glucose concentration (36), that the cerebral metabolic rates of glucose and oxygen as well as cerebral blood flow are fairly constant in the nonstimulated human brain (37–39), and that consistent T_{max}/V_{gly} ratios were obtained when fitting the data for each subject separately. The solid line in Fig. 3 represents the best fit of this model to the data, yielding K_t = 6.2 ± 1.7 mM and T_{max} = 1.2 ± 0.1 μmol/g·min.

With the localization technique used, we estimate the signal of glucose in blood to be attenuated relative to brain tissue due to reduced NOE generation. Nevertheless, if the measured brain glucose concentrations (Fig. 3) are reduced by the maximal contamination from vascular spaces in the occipital lobe—i.e., 5% (38, 39)—the derived kinetic constants are K_t = 5.6 ± 1.4 mM, which is not significantly different, and T_{max}/V_{gly} = 3.3 ± 0.2, which is reduced by 17% relative to the value in Fig. 3.

DISCUSSION

Glucose transport does not become rate-limiting to glycolysis until the intracellular glucose concentration falls into the range of the K_m of hexokinase, which is ≈50 μM (8), which is considerably lower than the brain glucose concentration of 1.0 ± 0.1 mM brain vol (mean ± SE; n = 6) measured at euglycemia. Glucose transport is therefore not rate-limiting in the normal human brain. This is consistent with the inflow rate T_{in} being at least 1.5 times the consumption rate V_{gly} at 5 mM plasma as calculated from the Michaelis–Menten expression for I_{in} using derived kinetic parameters of transport (see Fig. 3 legend). The plasma glucose concentration at which the brain levels approach zero was calculated to be 2.2 ± 0.5 mM. It is noteworthy that this is consistent with the level to which plasma glucose must be lowered in subjects to induce electrophysiological changes in the brain (40, 41).

The determination of brain glucose transport from the measured brain glucose concentrations has several advantages over other noninvasive techniques. Unidirectional transport rates can be assessed in humans by analyzing the time course of D-[^{11}C]glucose entering the brain using positron-emission tomography (PET) (11). Interpretation of such studies is difficult because, ideally, the measurement must be performed before significant amounts of radiolabel are incorporated into other metabolites where the signal cannot be distinguished from that of glucose. This limitation was overcome in our study by the direct, substrate-specific quantitation of D-[1-^{13}C]glucose at steady state by ^{13}C NMR. The use of the stable ^{13}C isotope also reduces the risks of such experiments in human studies. A fast isotopic turnover time is inferred from the fact that the euglycemic brain glucose concentration of 1.0 μmol/ml will be consumed in 3 min, based on a glycolytic rate of 0.3 μmol/g·min in the nonstimulated human brain (37), which may pose problems for PET measurements of D-[^{11}C]glucose transport that last 20 min (11). Glucose transport has also been estimated in one study using the nonmetabolizable glucose analog 3-*O*-[*methyl*-^{11}C]glucose, which reported K_t = 3.8 μmol/g and T_{max} = 1.9 μmol/g·min (42). However, using these constants with the symmetric Michaelis–Menten transport model (Eq. **1** in Fig. 3 legend) predict a brain glucose concentration that is twice the measured value at euglycemia (Fig. 3).

CONCLUSIONS

In conclusion, ^{13}C NMR permits direct quantitation of intracerebral glucose in humans. Transport kinetics can be derived from the measured brain glucose concentrations. The

measured kinetic constants in adolescents are consistent with glucose transport not being rate-limiting for metabolism until plasma levels drop to 2–3 mM. The ability to measure brain glucose concentration as a function of plasma provides the possibility of studying the regulation of glucose transport in the human brain *in vivo* in health and disease.

We acknowledge the support of the staff of both the Children's and General Clinical Research Centers: Mary Riordan, Louise Matthews, Patty Gatcomb, and Sarah Kerr. We also thank Peter Brown for the coil construction and Terry Nixon for maintaining and improving spectrometer performance. This work was supported by Grants RR06022, P01DK34576, R29NS28790, P01HD27757, and RR-00125-26 from the National Institutes of Health (Bethesda, MD) and by a grant from the Juvenile Diabetes Foundation International (E.J.N.).

1. Siesjö, B. K. (1978) *Brain Energy Metabolism* (Wiley, New York), pp. 110–117.
2. Pardridge, W. M. (1983) *Physiol. Rev.* **63,** 1481–1535.
3. Bachelard, H. S., Daniel, P. M., Love, E. R. & Pratt, O. E. (1973) *Proc. R. Soc. London Ser. B* **183,** 71–82.
4. Oldendorf, W. H. (1971) *Am. J. Physiol.* **221,** 1629–1639.
5. Mueckler, M., Caruso, C., Baldwin, S. A., Panico, M., Blench, I., Morris, H. R., Allard, W. J., Lienhard, G. E. & Lodish, H. F. (1985) *Science* **229,** 941–945.
6. Kalaria, R. N., Gravina, S. A., Schmidley, J. W., Perry, G. & Harik, S. I. (1988) *Ann. Neurol.* **24,** 757–764.
7. Pardridge, W. M., Boado, R. J. & Farrel, C. R. (1990) *J. Biol. Chem.* **265,** 18035–18040.
8. Lund-Andersen, H. (1979) *Physiol. Rev.* **59,** 305–352.
9. Gjedde, A. (1982) *Brain Res. Rev.* **4,** 237–274.
10. Fox, P. T., Raichle, M. E., Mintun, M. A. & Dence, C. (1988) *Science* **241,** 462–464.
11. Gutniak, M., Blomqvist, G., Widén, L., Stone-Elander, S., Hamberger, B. & Grill, V. (1990) *Am. J. Physiol.* **258,** E805–E812.
12. Agardh, C. D., Kalimo, H., Olsson, Y. & Siesjö, B. K. (1981) *J. Cereb. Blood Flow Metab.* **1,** 71–84.
13. Pramming, S., Thorsteinsson, B., Theilgaard, A., Pinner, B. M. & Binder, C. (1986) *Br. Med. J.* **292,** 647–650.
14. DeVivo, D. C., Trifiletti, R. R., Jacobson, R. I., Ronen, G. M., Behmand, R. A. & Harik, S. I. (1991) *N. Engl. J. Med.* **325,** 703–709.
15. Holden, J. E., Mori, K., Dienel, G. A., Cruz, N. F., Nelson, T. & Sokoloff, L. (1991) *J. Cereb. Blood Flow Metab.* **11,** 171–182.
16. Mason, G. F., Behar, K. L., Rothman, D. L. & Shulman, R. G. (1992) *J. Cereb. Blood Flow Metab.*, in press.
17. Pontén, S., Ratcheson, R. A., Salford, L. G. & Siesjö, B. K. (1973) *J. Neurochem.* **21,** 1127–1138.
18. Mies, G., Cruz, N. & Sokoloff, L. (1991) *J. Neurochem.* **56,** 1673–1676.
19. Luyten, P. R., Groen, J. P., Vermeulen, J. W. A. H. & den Hollander, J. A. (1989) *Magn. Reson. Med.* **11,** 1–21.
20. Tofts, P. S. & Wray, S. (1988) *NMR Biomed.* **1,** 1–10.
21. Williams, S. R. & Gadian, D. G. (1986) *Q. Rev. Exp. Physiol.* **71,** 335–360.
22. Radda, G. K., Rajagopalan, B. & Taylor, D. J. (1989) *Magn. Reson. Q.* **5,** 122–151.
23. Prichard, J. W. & Shulman, R. G. (1986) *Annu. Rev. Neurosci.* **9,** 61–85.
24. Behar, K. L., Petroff, O. A. C., Prichard, J. W., Alger, J. R. & Shulman, R. G. (1986) *Magn. Reson. Med.* **3,** 911–920.
25. DeFronzo, R. A., Tobin, J. E. & Andres, R. (1979) *Am. J. Physiol.* **237,** E214–E223.
26. Shulman, G. I., Rothman, D. L., Jue, T., Stein, P., deFronzo, R. A. & Shulman, R. G. (1990) *N. Engl. J. Med.* **322,** 223–228.
27. Bax, A. (1983) *J. Magn. Reson.* **52,** 76–80.
28. Gruetter, R. & Boesch, C. (1992) *J. Magn. Reson.* **96,** in press.
29. Ordidge, R. J., Connelly, A. & Lohman, J. A. B. (1986) *J. Magn. Reson.* **66,** 283–294.
30. Gruetter, R., Boesch, C., Martin, E. & Wüthrich, K. (1990) *NMR Biomed.* **3,** 265–271.
31. Lawry, T. J., Karczmar, G. S., Weiner, M. W. & Matson, G. B. (1989) *Magn. Reson. Med.* **9,** 299–314.
32. Shaka, A. J., Keeler, J. & Freeman, R. (1985) *J. Magn. Reson.* **53,** 313–340.
33. Bottomley, P. A., Hardy, C. J., Roemer, P. B. & Mueller, O. M. (1989) *Magn. Reson. Med.* **12,** 348–363.
34. Gjedde, A. & Diemer, N. H. (1983) *J. Cereb. Blood Flow Metab.* **3,** 303–310.
35. Press, W. H., Flannery, B. P., Teukolsky, S. A. & Vetterling, W. T. (1989) *Numerical Recipes in Pascal* (Cambridge Univ. Press, New York), pp. 572–590.
36. Pappenheimer, J. R. & Setchell, B. P. (1973) *J. Physiol. (London)* **233,** 529–551.
37. Tyler, J. L., Strother, S. C., Zatorre, R. J., Alivisatos, B., Worsley, K. J., Diksic, M. & Yamamoto, Y. L. (1988) *J. Nucl. Med.* **29,** 631–642.
38. Yamaguchi, T., Kanno, I., Uemura, K., Shishido, F., Inugami, A., Ogawa, T., Murakami, M. & Suzuki, K. (1986) *Stroke* **17,** 1220–1228.
39. Leenders, K. L., Perani, D., Lammertsma, A. A., Heather, J. D., Buckingham, P., Healy, H. J. R., Gibbs, J. M., Wise, R. J. S., Hatazawa, J., Herold, S., Beaney, R. P., Brooks, D. J., Spinks, T., Rhodes, C., Frackowiack, R. S. J. & Jones, T. (1990) *Brain* **113,** 27–47.
40. Hinzen, D. H. & Müller, U. (1971) *Pflügers Arch.* **322,** 47–52.
41. Creutzfeldt, O. D. & Meisch, J. J. (1963) *Electroencephalogr. Clin. Neurophysiol.* **24,** Suppl., 158–163.
42. Feinendegen, L. E., Herzog, H., Wieler, H., Patton, D. D. & Schmid, A. (1986) *J. Nucl. Med.* **27,** 1867–1877.